PROCEEDINGS of the
23rd International Congress on Acoustics

9 to 13 September 2019 in Aachen, Germany

Verification of Accuracy Using Measured Values of Low Frequency Noise Numerical Analysis Generated from Expressway Bridge

Hiroshi IWABUKI[1]; Osamu FUNAHASHI[2]; Masayuki SHIMURA[3]; Noboru KAMIAKITO[4]

[1] Nippon Expressway Research Institute Company Limited., Japan

[2] Nippon Expressway Research Institute Company Limited., Japan

[3] Civil Engineering And Eco-Technology Consultants Company Limited., Japan

[4] Civil Engineering And Eco-Technology Consultants Company Limited., Japan

ABSTRACT

In Japan, road managers including expressway may respond to complaints such as road traffic noise, vibration, low frequency noise, and so on from residents along the road. Among these countermeasures, noise and vibration and so on complaints are identified and countermeasures are further examined and constructed, but on the other hand, in the case of low frequency noise caused by bridges, many examinations on the occurrence mechanism are required. Therefore, in this study, unsteady analysis was proposed by three-dimensional finite element method on responses of a bridge due to vehicle load running on a bridge. The numerical simulation of the low frequency noise field was carried out by calculating the three dimensional wave equations with this unsteady analysis result as an unsteady boundary condition. By this method, it became possible to quantitatively investigate to which part of the bridge the cause of the low frequency noise originates. In this paper, identification of the cause of occurrence and simulation accuracy of the propagation path were verified by using the measured results of low frequency noise and vibration acceleration.

Keywords: Low Frequency Noise, Sound, Expressway Bridge, Numerical Analysis

1. INTRODUCTION

With the promotion of public works, environmental problems, especially low frequency noise problems may occur. In recent years, many low frequency noise problems have arisen in wind power facilities in each country, and guidelines are shown and operated in Australia, New Zealand, Canada and Norway. [1-8] In Japan, the Ministry of Environment has established the "Manual for measuring low-frequency sound" [9], and this manual has been in operation since October 2000. In this manual, it is shown that the generation mechanism of low frequency sound and the generation source according to the generation mechanism are a) due to flat plate vibration, b) due to pulsation of air flow, c) due to unsteady excitation of gas, d) rapid of air compression and release.

In Japan, the vibration of girders and slabs by the road traffic vibration spreads in the air, and produces low frequency noises in a land bridge particularly expressway bridge, and may receive a complaint from inhabitants to live in near expressways. It is necessary identifying an outbreak source and to examine an effective measures mechanic to cope with this complaint. What I install a lot of sensors in each part and material and belonging of the bridge, and many points measure at the same time is necessary, and there are great labor and the problem to cost of the expense in the preparations, measurement, analysis to measure the vibration of a figure and the floor version of the bridge, and to analyze it. It is intended that they estimate vibration and the quantity of the bridge by the simulation outbreak of the low frequency sound in substitution for the measurement in the true bridge, and the writers study technique analyzing the sound of the low frequency sound from dynamic reply analysis of the bridge upper part mechanic by the three dimensions finite element method to solve these. I became able to consider which part of the viaduct the cause of the low frequency sound was greatly

[1] h.iwabuki.aa@ri-nexco.co.jp
[2] o.funahashi.aa@ri-nexco.co.jp
[3] shimura@kensetsukankyo.co.jp
[4] kamiakit@kensetsukankyo.co.jp

caused by by past results of research [10] quantitatively. In this article, I report the result that examined identification of the origin and the simulation precision of the spread course using an actual survey result of a low frequency sound and the vibration acceleration.

2. Research bridge and conditions of measurement and analysis

Here, the outline of the bridge measured in this research, and the measurement conditions and analysis conditions are described.

2.1 Bridge outline

The target bridge of measurement and analysis of this research is 10 span continuous steel 2 main girder bridge among continuous viaducts. The main girder height is 4 m, the width is 10.9 m, the span length is 35 m, and a noise insulation wall with a height of 4 m is installed on the road shoulder side. A side view is shown in Fig. 1 and a cross-sectional view is shown in Fig.2

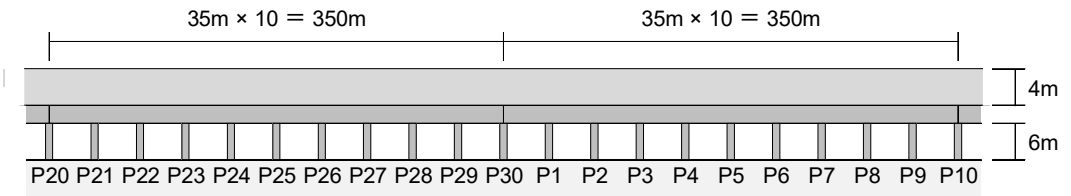

Fig.1 Side view

2.2 Measurement condition

Low frequency noise pressure levels were measured near the target bridge. The layout of the measurement points is shown in Fig.3and Fig.4. Four points were measured at a distance of 10 m from the bridge in the direction perpendicular to the bridge axis. In the bridge axis direction, S1 was set at P30, S2 was set at the middle of the span between P30 and P1, S3 was set at P1, and S4 was set at the middle of the span between P1 and P2. The measurement was performed at a sampling frequency of 200 Hz using a low frequency sound level meter NA-18 manufactured by RION.

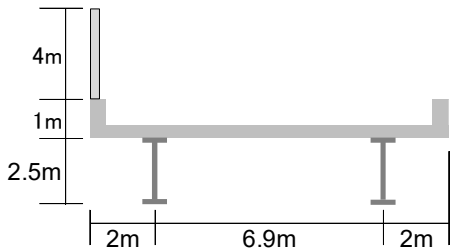

Fig.2 Cross-sectional view

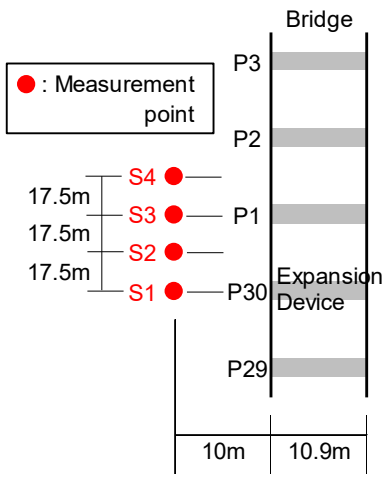

Fig.3 Plan view

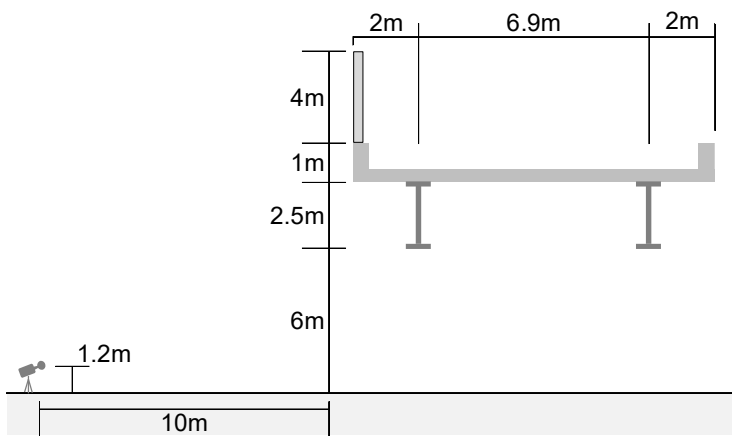

Fig.4 Cross-sectional view

2.3 Analysis condition

The sound field space to be analyzed covered four spans from P29 to P3 including the expansion device of P30. The dynamic response analysis of the bridge used the existing commercial code DALIA (KOZO KEIKAKU ENGINEERING Inc.). The motion equation was discretized by the finite element method, and time integration was sequentially performed on the unsteady external force (vehicle travel) to perform unsteady response analysis. By setting the vibration velocity waveform of the entire bridge calculated from the dynamic response analysis of the bridge as the load velocity, the sound field analysis is performed by FEM, with the entire bridge modeled in the dynamic response analysis as the target of sound pressure radiation. The conditions of the model were changed and analysis was performed in seven cases. Case 1 is the basis. Case 2, 3 and 4 were set in which the mesh spacing of Case 1 was changed. Cases 5, 6, and 7 were set in which the sound field space of Case 1 was changed. It is shown in Table 1. The analysis time was 5 seconds from the time when the vehicle passes P29.

Table.1 Analysis condition

item	Sound Field [m]			Mesh [m]		conditions
direction	x	y	z	x	z	
case 1	35	140	20	1	0.5	basis
case 2	35	140	20	2	0.5	Mesh: 2x in x direction
case 3	35	140	20	1	1	Mesh: 2x in z direction
case 4	35	140	20	1	2	Mesh: 4x in z direction
case 5	35	105	20	1	0.5	from P29 to P2
case 6	35	70	20	1	0.5	from P29 to P1
case 7	35	105	20	1	0.5	from P30 to P3

2.4 running conditions of the test vehicle

The measurement of low frequency noise was performed by driving a large test vehicle (Nissan Diesel: KL-CD48ZWH, 3-axis large vehicle, gross weight 245kN) with the general vehicle running excluded. The traveling position was in the traveling lane, and the traveling speed was 80 km / h. Analysis was performed by modeling this vehicle.

3. ANALYSIS METHOD OF LOW FREQUENCY NOISE

Here, a method of analyzing low frequency sound is described. In this research, in order to solve the dynamic response calculation of the structure by the three-dimensional finite element method and transmit it to the sound field space, the sound field analysis is also solved by the three-dimensional finite element method so that stress transfer of boundary conditions becomes easy. It was. [11] The excitation source was a driving excitation of a large test vehicle (Nissan Diesel: KL-CD48ZWH, 3-axle large vehicle, gross weight 245 kN) [12].

3.1 Primitive equation

In order to carry out the numeric simulation for the sound propagation in the air, the primitive variable equations are described in continuous system and equation of motion, as follows

$$\rho\frac{\partial u}{\partial t}+\frac{\partial p}{\partial x}=0 \quad \rho\frac{\partial v}{\partial t}+\frac{\partial p}{\partial y}=0 \quad \rho\frac{\partial w}{\partial t}+\frac{\partial p}{\partial z}=0 \tag{1}$$

$$\frac{\partial p}{\partial t}+\rho C^2\left(\frac{\partial u}{\partial x}+\frac{\partial v}{\partial y}+\frac{\partial w}{\partial z}\right)=0 \tag{2}$$

Where x, y, z are three dimensional coordinate system in space, and u, v, and w are acoustic

particulate velocity for each direction. While p, ρ, C and t are sound pressure, the density of air, sound speed and time respectively. Unknown parameters are u, v, w, and p.

3.2 Derivation of a wave equation

For efficient calculation, velocity potential φ is introduced to derive wave equation below with one unknown parameter, thus

$$p = \rho \frac{\partial \phi}{\partial t} \qquad u = -\frac{\partial \phi}{\partial x} \qquad v = -\frac{\partial \phi}{\partial y} \qquad w = -\frac{\partial \phi}{\partial z} \tag{3}$$

Where p is differentiated by time and u, v, and w are differentiated by each space coordinates. The derivative formulas become,

$$\frac{\partial p}{\partial t} = \rho \frac{\partial^2 \phi}{\partial t^2} \qquad \frac{\partial u}{\partial x} = -\frac{\partial^2 \phi}{\partial x^2} \qquad \frac{\partial v}{\partial y} = -\frac{\partial^2 \phi}{\partial y^2} \qquad \frac{\partial w}{\partial z} = -\frac{\partial^2 \phi}{\partial z^2} \tag{4}$$

Then wave equation can be obtained by substitute these equations into continuous system.

$$\frac{\partial^2 \phi}{\partial t^2} - C^2 \left(\frac{\partial^2 \phi}{\partial x^2} + \frac{\partial^2 \phi}{\partial y^2} + \frac{\partial^2 \phi}{\partial z^2} \right) = 0 \tag{5}$$

3.3 Finite element equation and Boundary condition

The finite element method is applied to the wave equation to obtain matrix equation. However, linear shape function is used for unknown values on the peak of hexahedral element.

3.3.1 Finite element equation

Finite element equation is described as follows

$$M \frac{\partial^2 \phi}{\partial t^2} + C^2 \left(S_{xx} + S_{yy} + S_{zz} \right) \phi = -C^2 N u_n \tag{6}$$

Then, each matrix is introduced by following integration

$$M = \int N_\alpha N_\beta d\Omega \qquad N = \int N_\alpha N_\beta d\Gamma \tag{7}$$

$$S_{xx} = \int \frac{\partial N_\alpha}{\partial x} \frac{\partial N_\beta}{\partial x} d\Omega \qquad S_{yy} = \int \frac{\partial N_\alpha}{\partial y} \frac{\partial N_\beta}{\partial y} d\Omega \qquad S_{zz} = \int \frac{\partial N_\alpha}{\partial z} \frac{\partial N_\beta}{\partial z} d\Omega \tag{8}$$

Where dΩ and dΓ are the analysis domain and the boundary, respectively.

3.3.2 Handling of a time differentiation clause

Time derivative of φ can be differentiated as follows,

$$\frac{\partial^2 \phi}{\partial t^2} = \frac{\phi^{m+1} - 2\phi^m + \phi^{m-1}}{\Delta t^2} \tag{9}$$

Where *m* means time step.

3.3.3 Boundary condition

* The definition for particle velocity (e.g. the slab plate, the sound barriers, and the back acoustic board) is given by

$$u_n = -\frac{\partial \phi}{\partial n} \tag{10}$$

* Sound penetration condition (i.e. impedance conditions÷ with open boundary) is presented by

$$u_n = \frac{p}{\rho C} = \rho \frac{\partial \phi}{\partial t} \frac{1}{\rho C} = \frac{1}{C} \frac{\partial \phi}{\partial t} \tag{11}$$

* Sound reflection condition (for solid surfaces, such as the ground surface and a building used as natural boundary conditions in FEM) can be defined as

$$u_n = -\frac{\partial \phi}{\partial n} = 0 \tag{12}$$

Where n is the normal direction of coordinate system.

With the application of lumped mass finite element equation, inverse-matrix calculation of M becomes unnecessary, thus improve calculation speed.

4. Analysis of measurements and results

4.1 Time history waveforms

The time history waveform of the measured value and the analyzed value is compared and analyzed. The respective time history waveforms of S1 to S4 are shown in Fig.5 to Fig.8.

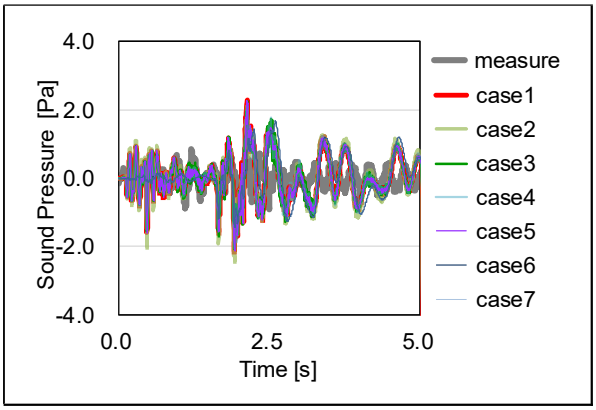

Fig.5 Time history waveforms of S1

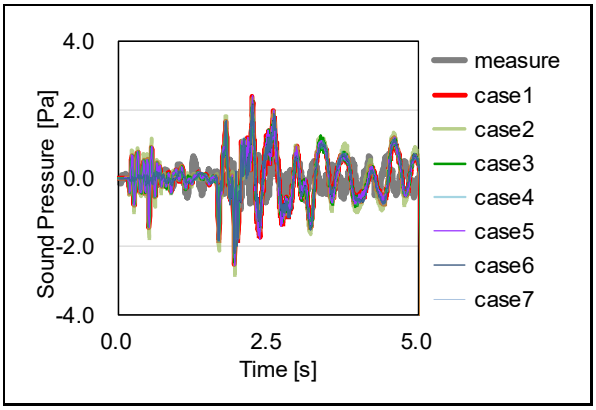

Fig.6 Time history waveforms of S2

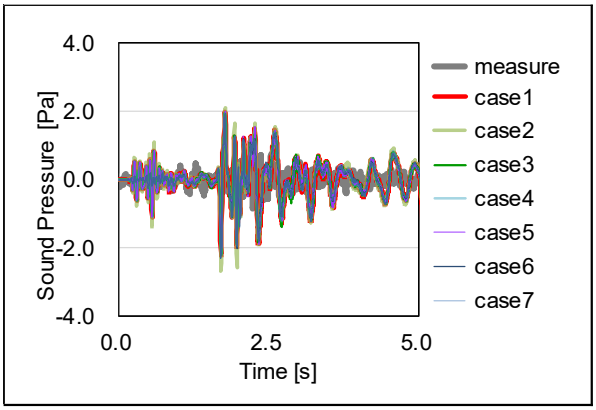

Fig.7 Time history waveforms of S3

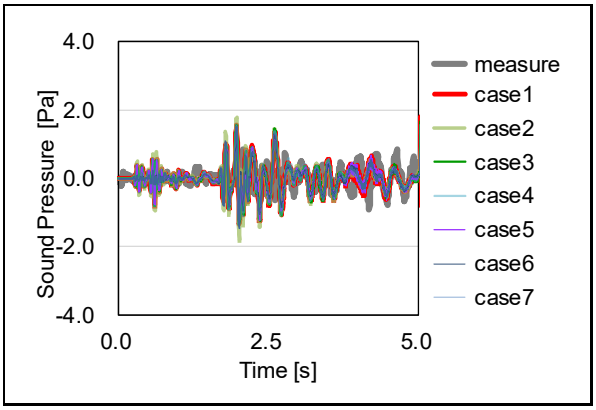

Fig.8 Time history waveforms of S4

The vehicle is reached at P30 (Time = 1.575[s]) having an expansion device, passing P29 (Time = 0.0 [s]). After that, it can be seen that the value of the low frequency noise increases. This tendency is also observed with measured values and analyzed values. In the analysis values, Case 2 and 4 tend

to have a slightly different amplitude. It is assumed that changing the mesh spacing in the direction perpendicular to the bridge axis has an influence on the amplitude. On the other hand, even if the mesh spacing in the bridge axis direction is changed, the influence on the amplitude is small. It is assumed that the contribution from the nearest bridge member is high, and that the low frequency sound propagates radially but has a certain directivity. On the other hand, no major difference is seen except Case 2. Therefore, even if the mesh spacing in the bridge axis direction is changed, the influence on the amplitude is small.

4.2 Frequency characteristics

The frequency characteristics were calculated by FFT analysis of time history waveform data. The condition of the FFT analysis was that the number of output points was 1,024 points, the window function was a Hamming function, the sampling time was 0.005 [s], and the frequency resolution was 0.0976625 [Hz]. The frequency characteristics were calculated under these conditions for both measured and analyzed values, and comparison and analysis were performed. In the vertical axis, the left side is the measured value, and the right side is the analyzed value.

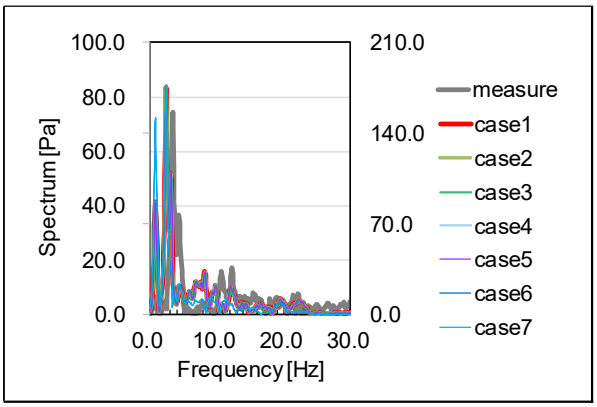

Fig.10 Frequency characteristics of S1

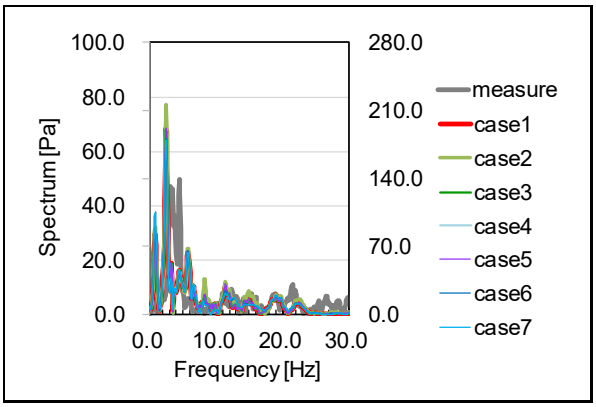

Fig.11 Frequency characteristics of S2

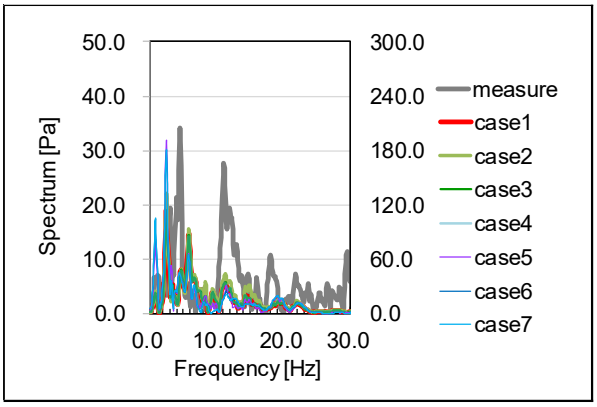

Fig.12 Frequency characteristics of S3

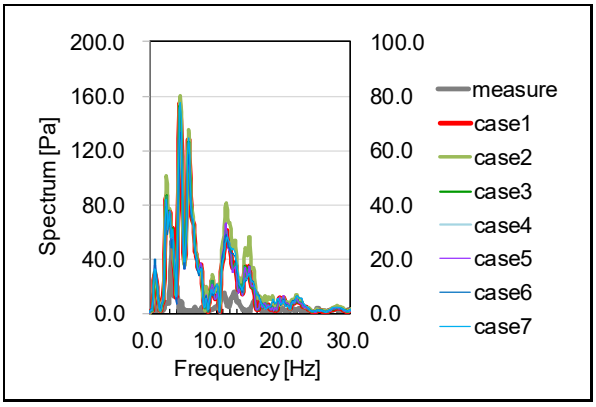

Fig.13 Frequency characteristics of S4

The respective frequency characteristics of S1 to S4 are shown in Fig 10 to Fig.13. The most prominent frequency is 3 to 4 [Hz] in the actual measurement value, while the analysis value is approximately 2 to 3 [Hz], though it is slightly smaller, but it is almost the same. Although the degree of excellence are different in the tens of Hz band, the peak values are almost the same. Focusing only on analysis, Case 2 shows slightly different characteristics from the other cases. This is similar to the time history waveform. Changing the mesh spacing in the direction perpendicular to the bridge axis affects the frequency characteristics, while changing the mesh spacing in the bridge axis direction reduces the effects on the frequency characteristics. Focusing only on analysis, S2 and S4 on the side of the center of the span have almost no difference in frequency characteristics in each case, while S1 and S3 on the side of the bridge pier have differences in frequency characteristics in each case. In an actual phenomenon, it is possible that structures such as girder ends, supports, and bridge piers

influenced the propagation of low frequency sound, and it is assumed that the analysis value deviates from the actual measurement value. Also, in the frequency band above 20 Hz, the analysis value tends to deviate from the measured value. It is conceivable that as the frequency band becomes higher, the wavelength becomes shorter, and when the mesh spacing is large, the waveform cannot be captured. In order to increase the accuracy of this frequency band by this method, it is considered necessary to reduce the mesh spacing.

From the above, the present method is in a situation where it is difficult to make the analysis value coincide with the measurement value at present, but it is possible to derive the tendency of the frequency characteristic of the measurement value from the analysis value. Therefore, environmental problems relating to low frequency noise occur, and it is considered to be effective in investigating the cause and taking measures.

5. CONCLUSIONS

In this paper, we developed a method to analyze the acoustics of low frequency noise with the aim of estimating the vibration and low frequency noise of the bridge by simulation without measuring the actual bridge. In addition, low frequency noise was measured when a test vehicle was run without a general vehicle traveling on a bridge in service, and the measurement results were compared with the analysis results. As a result, the following was shown.

- The actual measurement value and the analysis value by the present method differ in the degree of excellence of the amplitude value of the time history waveform and the frequency characteristic. However, almost the same tendency was obtained for the frequency characteristics. Therefore, it is considered effective in investigating the causes of environmental problems and taking measures.
- The mesh spacing of the sound field space needs to set the spacing necessary for analysis of the target frequency band.

These acquired findings are considered to be useful for coping with environmental problems that occur in various projects such as expressway projects.

In the future, it is an issue to expand the application range of this method by conducting similar analysis with different types of bridges.

ACKNOWLEDGEMENTS

In this research, the members of the Road Traffic Vibration Estimation Subcommittee of the Institute of Noise Control Engineering of Japan (INCE/J) received a great deal of cooperation in experiments and analysis. I express my gratitude to this.

REFERENCES

1. Environment Protection Authority：Wind Farms Environmental Noise Guidelines（2009）.
2. Technical Committee AV/5/6 Wind Turbine Generators for the Standards Council：NZS6808:1998 Acoustics - The assessment and measurement of sound from wind turbine generators（1998）.
3. STANDARDS AUSTRALIA Committee EV-016 -Acoustic-Wind Turbine Generator Noise：Australian Standard Acoustics -Measurement, prediction and assessment of noise from wind turbine generators（2007）.
4. Malcolm Hunt and Lindsay Hannah：The Use of Noise Perception Index (NPI) For Setting Wind Farm Noise Limits，3rd International Conference on Wind Turbine Noise （WTN2009）.
5. Ontario Ministry of Environment：Noise Guidelines for Wind Farms Interpretation for Applying MOE NPC Publications to Wind Power Generation Facilities （2008）.
6. Ontario Ministry of Environment ： Development of Noise Setbacks for Wind Farms-Requirements for Compliance with MOE Noise Limits（2009）.
7. International Organization for Standardization：ISO 9613-2:1996 Acoustics -Attenuation of sound during propagation outdoors -Part 2: General method of calculation（1996）.
8. Sigurd Solberg and Inge Hommedal：A critical look at the wind turbine noise regime in Norway，3rd International Conference on Wind Turbine Noise （WTN 2009）.

9. Manual on how to measure low frequency sound : Ministry of Environment, 2000.10.
10. Hiroshi Iwabuki , Toshikazu Osafune , Masayuki Shimura , and Noboru Kamiakito , Atsushi Aoki , Masato Kobayashi , and Hisashi Niwa : Numerical simulation for low frequency sound emitted from viaduct of the road by the vehicle load, internoise2013, paper0955 (2013)
11. T. Nomura, K. Takagi and S. Sato, “Finite element simulation of sound propagation concerning meteorological conditions”. International Journal for Numerical Methods in Fluids, 2010, vol.64:1296-1318
12. Saiji Fukada, Kimihisa Usui, Yasuo Kajikawa and Masahiko Harada “Simulation of vibration and sound characteristics occurred from extended deck bridges with various skew due to running vehicle” Structure Engineering in Japan Vol.53A,pp.287-298,2007.3